

# Thermolides, Potent Nematocidal PKS-NRPS Hybrid Metabolites from Thermophilic Fungus *Talaromyces thermophilus*

Ji-Peng Guo,<sup>†</sup> Chun-Yan Zhu,<sup>†</sup> Chuan-Ping Zhang,<sup>†</sup> Yan-Sheng Chu,<sup>†</sup> Yan-Li Wang, Jun-Xian Zhang, De-Kai Wu, Ke-Qin Zhang,\* and Xue-Mei Niu\*

Laboratory for Conservation and Utilization of Bio-Resources & Key Laboratory for Microbial Resources of the Ministry of Education, Yunnan University, Kunming 650091, P. R. China

**S** Supporting Information

**ABSTRACT:** Macrocyclic PKS-NRPS hybrid metabolites represent a unique family of natural products mainly from bacteria with broad and outstanding biological activities. However, their distribution in fungi has rarely been reported, and little has been reported regarding their nematocidal activity. Here we describe an unprecedented class of PKS-NRPS hybrid metabolites possessing a 13-membered lactam-bearing macrolactone, thermolides A–F (1–6) from a thermophilic fungus *Talaromyces thermophilus*. We showed that 1 and 2 displayed potent inhibitory activity against three notorious nematodes with LC<sub>50</sub> values of 0.5–1 μg/mL, as active as commercial avermectins. This work provided a new class of promising lead compounds for nematocide discovery.

Nematodes are among the most abundant multicellular animals on earth, and phytoparasitic nematodes are among the most notoriously difficult crop and wood pests to control.<sup>1</sup> Due to concerns about public health and environmental safety, chemical nematocides such as organophosphate and carbamate insecticides are being withdrawn from the market. In the past 20 years, only a small repertoire of agents, mainly avermectins, have arisen to address the growing need for nematode control.<sup>2,3</sup> Nematodes also are distinguished as useful tools for the discovery of novel drugs because several human disease models have been built in the *Caenorhabditis elegans*.<sup>4</sup>

Macrocyclic PKS-NRPS hybrid metabolites are a unique family of natural products from microorganisms, mainly from bacteria.<sup>5</sup> They display a wide range of impressive biological activities and include the immunosuppressant rapamycin, the anticancer agent epothilone, the pristinamycin components of the antibiotic synergid, the ansa antibiotics including the antitubercular drugs of the rifamycin group, the Hsp90 inhibitor geldanamycin, and the maytansine family antitumor agent ansamitocin.<sup>6,7</sup> Moreover, the products of the PKS-NRPS pathways present a large pool of novel chemical entities that have been selected during evolution by providing an advantage to the producer/host.<sup>8</sup> Nevertheless, their distribution in fungi has not been well investigated, and no work has been reported about their application as nematocidal agents.<sup>9</sup>

Thermophilic fungi are eukaryotes that thrive at high temperatures. They represent a potential reservoir of thermostable enzymes for industrial applications and could be developed into cell factories to support the production of

chemicals and materials at elevated temperatures.<sup>10</sup> However, very few of them have been screened for their production of structurally and biologically novel secondary metabolites.<sup>11</sup> Recently, we found that a thermophilic fungus *Talaromyces thermophilus*, collected from the Tengchong hot spring of Yunnan, China, could produce two putative key biosynthetic intermediates, talathermophilins A and B,<sup>12</sup> which had long been proposed for the biosynthesis of crenulated tryptophan alkaloids but never really isolated and identified. Continuing work on the fungus resulted in the discovery of the precursors for the postulated biosynthetic pathways for talathermophilins.<sup>13</sup>

In our further investigations on the metabolic profiles of thermophilic fungi collected from the same habitat, a novel class of PKS-NRPS hybrid molecules was obtained from the thermophilic fungus *T. thermophilus* YM 3-4. These metabolites possess a 13-membered lactam-bearing macrolactone and are shown as thermolides A–F (1–6) in Figure 1. Interestingly, compounds 1 and 2 were found to show potent inhibitory activity against three notorious nematodes.

Thermolides A–C (1–3) were obtained as major constituents among these metabolites from the culture broths of *T. thermophilus*. They all exhibited a quasi-molecular ion peak at *m/z* 544 [M–H]<sup>–</sup> in their negative ESI spectra and were

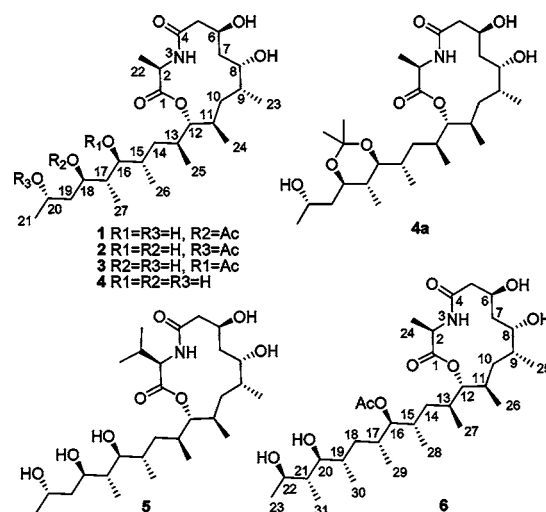


Figure 1. Structures of 1–6 and 4a.

Received: October 21, 2012

Published: December 4, 2012

assigned to a molecular formula of  $C_{28}H_{51}NO_9$ , on the basis of HRESIMS and NMR data (Table S1).

The  $^1H$  NMR spectrum of **1** displayed obvious signals for seven secondary methyl groups ( $\delta_H$  1.28, 1.11, 0.98, 0.95, 0.87, 0.85, and 0.79), one tertiary methyl of an acetoxy group ( $\delta_H$  1.96), six O-bearing methines, and one N-bearing methine ( $\delta_H$  5.46, 4.75, 4.57, 4.23, 3.73, 3.55, and 3.25). The  $^{13}C$  NMR and DEPT spectra of **1** indicated signals attributable to three carbonyl groups ( $\delta_C$  169.8, 171.1, and 172.6), twelve methines (including six O-bearing ones), five methylenes, and eight methyl groups. The presence of the three carbonyl groups accounted for 3 of 4 sites of unsaturation, suggesting the existence of one ring in **1**. The HSQC spectrum of **1** enabled the assignment of all H-atoms to the directly bonded C-atoms.

Interpretation of the  $^1H$ - $^1H$  COSY spectrum of **1** led to the unambiguous establishment of three segments, the moieties H2/Me22 (A), H<sub>2</sub>5/H6/H<sub>2</sub>7/H8 (B), and H16/H17(Me27)/H18/H<sub>2</sub>19/H<sub>2</sub>20/Me21 (C) (Figure 2) due to the congested proton

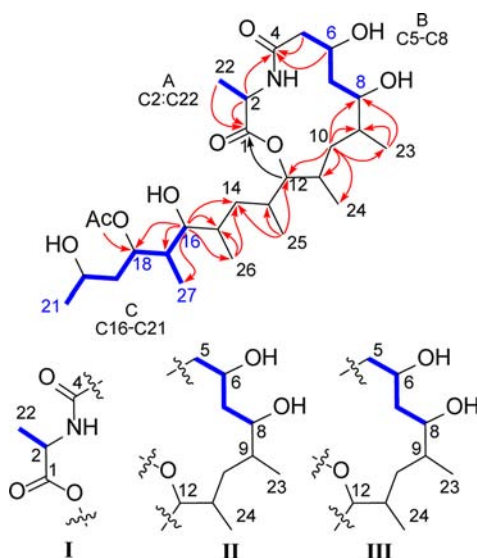


**Figure 2.** Key correlations in  $^1H$ - $^1H$  COSY (bold blue bonds) and HMBC spectra (red curves) leading to partial chemical substructures and eventually the planar structure of **1**.

signals ranging from  $\delta_H$  1.80–1.65 ascribable to three methines ( $\delta_C$  34.9, 33.1, and 32.1). The HMBC correlations of H2 at  $\delta_H$  4.75 with two carbonyl carbons at  $\delta_C$  172.6 (C1) and 169.8 (C4), and the methyl carbon at  $\delta_C$  16.7 (C22), and of Me22 at  $\delta_H$  1.28 with C1 and one methine carbon at  $\delta_C$  47.4 (C2) (Figure 2), together with one nitrogen in the molecular formula, led to elucidation of moiety I derived from segment A. Similarly, moiety II derived from segment B were deduced by the HMBC correlations of H10 at  $\delta_H$  1.38 with two methine carbons at  $\delta_C$  34.9 (C9) and  $\delta_C$  31.0 (C11), two methyl carbons at  $\delta_C$  17.1 (C23) and 17.4 (C24), two oxymethine carbons at  $\delta_C$  75.9 (C8) and at 84.4 (C12), and of Me23 at  $\delta_H$  0.98 with C8 and C9, combining with the above segment B. The strong HMBC correlations of H12 at  $\delta_H$  4.58 with C1 and of H5 at  $\delta_H$  2.57 and H6 at  $\delta_H$  4.23 with C4 were the key correlations to determine the linkage of moieties I and II to complete an unprecedented 13-membered macrocyclic core bearing one lactam, accounting for the remaining site of unsaturation. The downfield shifted chemical value of H18 at  $\delta_H$  5.46 suggested that the only acetoxy group was attached to C18 at  $\delta_C$  73.4, which was further supported by a strong correlation between H18 and the acetyl

carbonyl carbon at  $\delta_C$  171.1 in the HMBC spectrum. The HMBC correlations of H16 with two methine carbons at  $\delta_C$  33.1 (C15) and 39.9 (C17), two methyl carbons at  $\delta_C$  17.5 (C26) and 12.6 (C27), one methylene carbon at  $\delta_C$  33.6 (C14), and C18 allowed us to establish partial substructure III derived from segment C. This assignment was supported by the  $^1H$ - $^{13}C$  long-range correlations from Me26 to C14/C15/C16. The  $^1H$ - $^1H$  correlation of the methyl at  $\delta_H$  0.79 (Me25) with H13 at  $\delta_H$  1.78 and HMBC correlations from Me25 to C13/C12/C14 allowed for incorporation of the last methine C13 into the structure, which served as a bridge to connect the macrocyclic core and the partial substructure III to form the whole planar structure of **1**.

Compounds **2**–**3** shared the same 13-membered macrocyclic core as **1** deduced by the analysis of NMR spectrometric data (Table S1). The chemical values of H20 in **2** and H16 in **3** were downshifted to  $\delta_C$  5.09 and 4.76, respectively, and revealed that the acetyl group was linked to C20 in **2** and C16 in **3**, respectively. Thermolide D (**4**) was assigned to a molecular formula of  $C_{26}H_{49}NO_8$  on the basis of HRESI spectra. Analysis of NMR spectrometric data of **4** (Table S1) revealed that **4** was just a deacetyl derivative of **1**–**3**.

Thus, **1**–**4** feature a novel class of hybrid metabolites of an unprecedented 13-membered lactam-bearing macrolide linked to a saturated side chain with an ordered arrangement of methyls and hydroxyls, which together incorporate seven secondary methyl groups and five oxygenated groups at C6, C8, C16, C18, and C20. The stereochemistry of these metabolites was segregated into two distinct macrocyclic and side chain clusters.

Only one acetone derivative (**4a**) of **4** was obtained in this study, which was assigned to a molecular formula of  $C_{29}H_{53}NO_8$ . The 1D and 2D NMR spectrometric data (Table S2) revealed that **4a** was a 16,18 acetone derivative of **4**. The fact that acetone derivatization occurred at C16/C18 in **4**, where the steric hindrance was comparatively larger than that at C18/C20 and C6/C8, led to the arbitrary deduction of two moieties of 6,8-*anti*-diols and 16,18,20-*syn-syn-anti* triols in **1**–**4**. The *anti* configuration of the 6,8-diol moiety was in agreement with the absence of a NOE contact between H8 and H6 in the ROESY spectra of **1**–**4**.

The ROESY experiments for the side chain in **4a** displayed a strong 1,3-diaxial NOE correlation between H16 and H18, illustrating a preferable chair conformation of the six-membered ring where the hydroxyl groups at C16 and C18 were both in equatorial positions. The NOE contacts from Me27 to H16 and H18 suggested that H17 was also axial, which was confirmed by the vicinal coupling constant ( $J = 8.8$  Hz) between H16 and H17. The NOE contacts from H14a to H17, H16 to Me26, and H15 to Me27, indicated the stereochemistry of the C15 stereocenter was the same as that of C16. The small coupling constant ( $J = 2.0$  Hz) between H16 and H15 supported this deduction. The NOE correlations of OH20 to H18, and Me21 to H19b, together with a strong NOE contact between H20 and H19a, displayed that the stereochemistry of the C20 stereocenter was opposite to that of C18 (Figure 3).

Due to rotameric restrictions imposed by the 13-membered macrocyclic core and the 6-membered ring, a 1,3-*anti* relationship between C13 and C15 could be assigned on the basis of the strong NOE correlations of H13 to Me26, H14b to Me25, H14a to Me26, and H15 to Me25 in **4a** (Figure 3). Further evidence came from the large coupling constants ( $J = 13.0$  Hz) for H14a/H13 and H14b/H15 in the  $^1H$  NMR spectrum of the 6,20-*bis*-

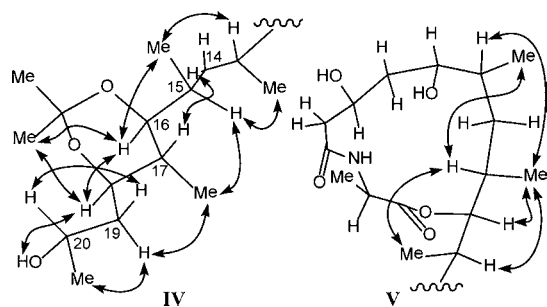


**Figure 3.** Selected key NOE contacts for the C13–C19 side chain (IV) and the C1–C13 macrolactone region (V).

MTPA derivative (**4R2**) of **4** (Table S4), while the signals for H<sub>2</sub>14 in **1–4** and **4a** were overlapped.

NMR methods alone are insufficient to unambiguously define the remaining stereochemical permutations. We attempted to solve the configuration of the thermolides through preparation and <sup>1</sup>H NMR analysis of the corresponding *-(R)-* and *-(S)-*MTPA ester derivatives of **4**.

The *R* and *S* penta-MTPA esters (**4R5** and **4S5**) were prepared from **4**, and the respective <sup>1</sup>H NMR signals (Table S3) were assigned from HSQC spectra. Mosher's analysis of negative  $\Delta\delta^{\text{SR}}$  ( $\delta\text{S}-\delta\text{R}$ ) of the *R* and *S* penta-MTPA esters in the region of H<sub>2</sub>–H<sub>11</sub> conformed with the 1,3-*anti*-diols model<sup>14,15</sup> and allowed assignment of 6*S* and 8*S*. The analysis of the 1,3,5-triol moiety was carried out by examination of pairwise additive anisotropic shifts in MTPA esters of 1,3-*syn*-diols and 3,5-*anti*-diols in accordance with the interpretation of Riguera et al.<sup>14,15</sup> for MTPA esters of diols and of Molinski et al.<sup>16,17</sup> for MTPA esters of *syn-syn-anti* triols (Table S3; Figures S1 and S2). The characteristic positive  $\Delta\delta^{\text{SR}}$  ( $\delta\text{S}-\delta\text{R}$ ) values for H<sub>13</sub>–H<sub>21</sub> supported the 16*S*,18*R*,20*S* configurations.

The stereochemistry of C<sub>9</sub>–C<sub>12</sub> in the macrocyclic cores of **1–4** was established with the help of the <sup>1</sup>H NMR and ROESY experiments for **4R5** due to its rotameric restrictions imposed by large MTPA groups. The broad singlet for H<sub>8</sub> in **4R5**, in combination with the absence of an NOE contact between H<sub>8</sub> and Me<sub>23</sub> in the ROESY spectrum of **4R5**, indicated a *syn* configuration at C<sub>8</sub>/C<sub>9</sub>. A partial MTPA derivatization experiment in which MTPA esterification of the macrocyclic core in **4** occurred initially at C<sub>6</sub> (6,20-*bis*-MTPA esters of **4**, **4R2**) further implied the existence of a steric-hindrance effect at C<sub>8</sub> caused by Me<sub>23</sub> residing on the same side as the OH<sub>8</sub> (Figure 3).

The strong NOE contacts between H<sub>9</sub> and Me<sub>24</sub> and between Me<sub>23</sub> and H<sub>11</sub> in the ROESY spectrum of **4R5** indicated a 1,3-*trans* configuration at C<sub>9</sub>/C<sub>11</sub> (Figure 3). The observation of a strong NOE correlation between H<sub>12</sub> and Me<sub>24</sub> suggested a *trans*-configuration for C<sub>11</sub>/C<sub>12</sub> with the two H-atoms H<sub>11</sub>/H<sub>12</sub> in a quasibisaxial conformation. The vicinal coupling constants ( $J = 7.6\text{--}8.3$  and  $3.2\text{--}3.8$  Hz) of H<sub>12</sub> signals in the <sup>1</sup>H NMR spectra of **1–4**, together with the key NOE correlations of Me<sub>24</sub> to H<sub>13</sub>, Me<sub>25</sub> to H<sub>11</sub>, and H<sub>14</sub> to H<sub>11</sub>, in combination with the absence of NOE contacts of Me<sub>24</sub> to Me<sub>25</sub> in the ROESY spectrum of **4R5**, confirmed the stereochemistry of C<sub>13</sub> deduced from a 1,3-*anti* relationship between C<sub>13</sub> and C<sub>15</sub>.

Acidic hydrolysis of **4**, followed by treatment with Marfey's reagent and analysis by HPLC,<sup>18,19</sup> showed the presence of D-alanine in **4**. The configurations of the C<sub>1</sub>–C<sub>12</sub> macrocyclic core and C<sub>13</sub>–C<sub>21</sub> chains have thus been established as shown in **4a** (Figure 1). The energy-minimized conformer **4aa** provided by

molecular modeling for **4a** (Supporting Information)<sup>20,21</sup> was in good agreement with the above deduction.

For the first congener of **4**, thermolide E (**5**) was assigned a molecular formula of C<sub>28</sub>H<sub>53</sub>NO<sub>8</sub> according to HRESIMS and NMR spectroscopy (Table S2). The signal characteristic for Me<sub>22</sub> at  $\delta_{\text{H}}$  1.29 in the <sup>1</sup>H NMR spectrum of **4** was missing while two geminal secondary methyls existed in the higher field region of the <sup>1</sup>H NMR spectrum of **5**. The diagnostic C<sub>2</sub> at  $\delta_{\text{H}}$  48.4 in **4** appeared downfield at  $\delta_{\text{C}}$  58.5 in **5**. The correlations in <sup>1</sup>H–<sup>1</sup>H COSY, HSQC, and HMBC spectra suggested that D-alanine in **4** was replaced by D-valine in **5**.

The HRESIMS analysis of thermolide F (**6**) established a molecular formula of C<sub>32</sub>H<sub>59</sub>NO<sub>9</sub>. The NMR data (Table S2) displayed that the carbon scaffold of **6** shared the same macrolactone core as **1–4** but possessed a C<sub>11</sub> side chain with penta-methyl groups and similar oxygenation pattern to **3**. The absolute configurations at the stereogenic centers in the C<sub>1</sub>–C<sub>13</sub> macrocyclic core in **6** were established to be identical to the corresponding parts in **1–5**, as similar NOE correlations in the regions of H<sub>2</sub>–H<sub>13</sub> were observed in the ROESY spectra. However, the assignment of the stereochemistry of the side chain in **6** was tricky due to the overlap of key signals. As derivatization experiments were hampered by the minute yields of **6** (0.7 mg), we sought to obtain clues with respect to its cometabolites **1–5**. It is interesting to note that not only the C<sub>1</sub>–C<sub>17</sub> substructure in **6** was the same as that in **3** (Blue square in Figure 4) but also the

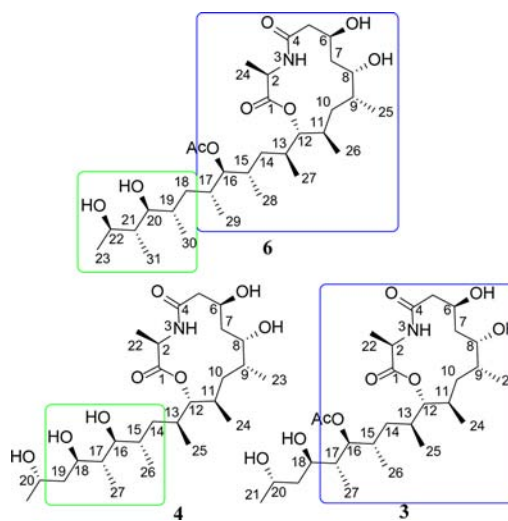


**Figure 4.** Analysis for the structural similarity of **3**, **4**, and **6**.

C<sub>18</sub>–C<sub>23</sub> moiety with a 1,3-dihydroxy-2,4-dimethyl substitution pattern in **6** was identical to the C<sub>14</sub>–C<sub>19</sub> regions in **4** (green square in Figure 4). Thus, the configurations of the C<sub>18</sub>–C<sub>23</sub> regions in **6** are tentatively determined to be identical to those of the C<sub>14</sub>–C<sub>19</sub> regions in **4**.

From the biosynthetic point of view, the macrolide cores in **1–6** could be formed by the linkage of one polyketide chain and one amino acid. The macrolide core consisting of one lactone and one lactam could be also found in the structures of unusual metabolites including rapamycin, an unusual PKS-NRPS hybrid metabolite bearing a 31-membered macrolide core, isolated from the bacterium *Streptomyces hygrosopicus*,<sup>6,7</sup> divergolides from an endophytic *Streptomyces* sp. HKI0576 of the mangrove tree *Bruguiera gymnorrhiza*,<sup>22</sup> and myxovirescins from gliding bacterium *Myxococcus xanthus* DK1622.<sup>23</sup> However, one amino acid involved in the formation of both the lactone and lactam is

not observed in these macrolide-core bearing compounds. To the best of our knowledge, this is the first report on the discovery of hybrid macrolides from a fungus origin. This finding may provide a new impetus for delineating the regulatory mechanism governing the variability in fungal metabolites and shed new light onto the unexplored biosynthetic abilities of unprecedented secondary metabolites in extremophilic fungi.

Compounds **1–4** were evaluated for their nematodetoxic activities against three types of nematodes including the root knot nematode *Meloidogyne incognita*, pine-wood nematode *Bursaphelenches siylophilus*, and free-living nematode *Panagrellus redivevus*.<sup>12</sup> **1** and **2** showed the strongest activities against all the worms with LC<sub>50</sub> values 0.5–1.0 μg/mL, similar to those of avermectins. **3** displayed moderate activity, and a weak inhibitory effect on the worms was observed for **4** (Table 1). Taken

**Table 1. Nematodetoxic Activities (LC<sub>50</sub>, μg/mL) of Thermolides A–D (1–4)**

compd	test nematode		
	<i>M. incognita</i>	<i>B. siylophilus</i>	<i>P. redivevus</i>
<b>1</b>	0.8	1.0	0.6
<b>2</b>	0.7	0.9	0.5
<b>3</b>	30.5	25.6	40.8
<b>4</b>	55.6	48.4	56.9
avermectins	0.7	0.5	0.8

together, **1–2** covered a range of nematode toxic activities. Investigation on the biosynthesis of the unique class of metabolites in the extremophilic fungus is currently underway in our laboratory.

In conclusion, we have isolated and characterized a novel class of potent nematocidal thermolides from a thermophilic fungus *T. thermophilus*. Thermolides A–F feature unprecedented PKS-NRPS hybrid metabolites containing a 13-membered lactam-bearing macrolactone and represent an exciting new class of promising leads for nematocidal agent discovery.

## ■ ASSOCIATED CONTENT

### Supporting Information

A description of experimental procedures, materials, extraction and isolation of seven compounds, bioassays of thermolides, crucial data (ORD, UV, IR, MS, <sup>1</sup>H, and <sup>13</sup>C NMR) and <sup>1</sup>H and <sup>13</sup>C NMR, COSY, HSQC, HMBC, and ROESY spectra of **1–6** and **4a**, and <sup>1</sup>H, <sup>13</sup>C spectra of the R and S MTPA esters of **4** were included. This material is available free of charge via the Internet at <http://pubs.acs.org>.

## ■ AUTHOR INFORMATION

### Corresponding Author

niuxm@yahoo.com; kqzhang1@yahoo.com.cn

### Author Contributions

<sup>†</sup>J.-P.G., C.-Y.Z., C.-P.Z., and Y.-S.C. contributed equally.

### Notes

The authors declare no competing financial interest.

## ■ ACKNOWLEDGMENTS

We thank Miss Hui-Min Xu and Dr. Yu Zhang at Kunming Institute of Botany of CAS for Merfay's reaction and molecular modeling, respectively, Prof. Hong-Bin Zhang for Mosher reaction, and Prof. Joan Bennett for editing. Financial support from NBRPC (973 Program, 2013CB127505), NHTRDPC

(2011AA10A205), NSFC (31070051 and U1036602), YATLR-FYP (2009CI051), CNTC (110201002023), and YBCTIC (2010YN17) is gratefully acknowledged.

## ■ REFERENCES

- (1) Kikuchi, T.; Cotton, J. A.; Dalzell, J. J.; Hasegawa, K.; Kanzaki, N.; McVeigh, P.; Takahashi, T.; Tsai, I. J.; Assefa, S. A.; Cock, P. J. A.; Otto, T. D.; Hunt, M.; Reid, A. J.; Sanchez-Flores, A.; Tsuchihara, A.; Yokoi, T.; Larsson, M. C.; Miwa, J.; Maule, A. G.; Sahashi, N.; Jones, J. T.; Berriman, M. *PLoS Pathog.* **2011**, *7*, e1002219.
- (2) Abad, P.; Gouzy, J.; Jean-Marc Aury; Castagnone-Sereno, P.; Danchin, E. G. J.; Deleury, E.; Perfus-Barbeoch, L.; Anthouard, V.; Artiguenave, F.; Blok, V. C.; Marie-Cécile Caillaud; Coutinho, P. M.; Dasilva, C.; Luca, F. D.; Deau, F.; Esquibet, M.; Flutre, T.; Goldstone, J. V.; Hamamouch, N.; Hewezi, T.; Jaillon, O.; Jubin, C.; Leonetti, P.; Magliano, M.; Maier, T. R.; Markov, G. V.; McVeigh, P.; Pesole, G.; Poulain, J.; Robinson-Rechavi, M.; Sallet, E.; Séguens, B.; Steinbach, D.; Tytgat, T.; Ugarte, E.; van Ghelder, C.; Veronico, P.; Baum, T. J.; Blaxter, M.; Bleve-Zacheo, T.; Davis, E. L.; Ewbank, J. J.; Favery, B.; Grenier, E.; Henrissat, B.; Jones, J. T.; Laudet, V.; Maule, A. G.; Quesneville, H.; Marie-Noëlle Rosso; Schiex, T.; Smant, G.; Weissenbach, J.; Wincker, P. *Nat. Biotechnol.* **2008**, *26*, 909.
- (3) Opperman, C. H.; Bird, D. M.; Williamson, V. M.; Rokhsar, D. S.; Burke, M.; Cohna, J.; Cromera, J.; Dienera, S.; Gajana, J.; Grahama, S.; Houfek, T. D.; Liu, Q.; Mitros, T.; Schaff, J.; Schaffer, R.; Scholl, E.; Sosinski, B. R.; Thomas, V. P.; Windham, E. *Proc. Natl. Acad. Sci. U.S.A.* **2008**, *105*, 14802.
- (4) Burns, A. R.; Wallace, I. M.; Wildenhain, J.; Tyers, M.; Giaever, G.; Bader, G. D.; Nislow, C.; Cutler, S. R.; Roy, P. J. *Nat. Chem. Biol.* **2010**, *6*, 549.
- (5) Walsh, C. T. *Science* **2004**, *303*, 1805.
- (6) Fischbach, M. A.; Walsh, C. T. *Chem. Rev.* **2006**, *106*, 3468.
- (7) Hertweck, C. *Angew. Chem., Int. Ed.* **2009**, *48*, 4688.
- (8) Mander, L.; Liu, H.-W. In *Comprehensive Natural Products II: Chemistry and Biology*, Vol. 5; Rath, C. M., Scaglione, J. B., Kittendorf, J. D., Sherman, D. H., Eds.; Elsevier: Oxford, 2010; pp 453.
- (9) Song, Z.; Cox, R. J.; Lazarus, C. M.; Simpson, T. J. *ChemBioChem* **2004**, *5*, 1196.
- (10) Berka, R. M.; Grigoriev, I. V.; Otilar, R.; Salamov, A.; Grimwood, J.; Reid, I.; Ishmael, N.; John, T.; Darmond, C.; Moisan, M.-C.; Henrissat, B.; Coutinho, P. M.; Lombard, V.; Natvig, D. O.; Lindquist, E.; Schmutz, J.; Lucas, S.; Harris, P.; Powlowski, J.; Bellemare, A.; Taylor, D.; Butler, G.; de Vries, R. P.; Allijn, I. E.; van den Brink, J.; Ushinsky, S.; Storms, R.; Powell, A. J.; Paulsen, I. T.; Elbourne, L. D. H.; Baker, S. E.; Magnuson, J.; LaBoissiere, S.; Clutterbuck, A. J.; Martinez, D.; Wogulic, M.; de Leon, A. L.; Rey, M. W.; Tsang, A. *Nat. Biotechnol.* **2011**, *29*, 922.
- (11) Wilson, Z. E.; Brimble, M. A. *Nat. Prod. Rep.* **2009**, *26*, 44–71.
- (12) Chu, Y. S.; Niu, X. M.; Wang, Y. L.; Guo, J. P.; Pan, W. Z.; Huang, X. W.; Zhang, K. Q. *Org. Lett.* **2010**, *12*, 4356.
- (13) Guo, J. P.; Tan, J. L.; Wang, Y. L.; Wu, H. Y.; Zhang, C. P.; Niu, X. M.; Pan, W. Z.; Huang, X. W.; Zhang, K. Q. *J. Nat. Prod.* **2011**, *74*, 2278.
- (14) Seco, J. M.; Martino, M.; Quiñoá, E.; Riguera, R. *Org. Lett.* **2000**, *2*, 3261.
- (15) Seco, J. M.; Quiñoá, E.; Riguera, R. *Chem. Rev.* **2004**, *104*, 17.
- (16) MacMillan, J. B.; Molinski, T. F. *Org. Lett.* **2002**, *4*, 1535.
- (17) Seco, J. M.; Quiñoá, E.; Riguera, R. *Chem. Rev.* **2012**, *112*, 4603.
- (18) Marfey, P.; Ottesen, M. *Carl. Res. Commun.* **1984**, *49*, 591.
- (19) Han, J.; Ji, C.-J.; He, W.-J.; Shen, Y.; Leng, Y.; Xu, W.-Y.; Fan, J.-T.; Zeng, G.-Z.; Kong, L.-D.; Tan, N.-H. *J. Nat. Prod.* **2011**, *74*, 2571.
- (20) Paterson, I.; Dalby, S. M.; Roberts, J. C.; Naylor, G. J.; Esther, A. G.; Isbrucker, R.; Pitts, T. P.; Linley, P.; Divlianska, D.; Reed, J. K.; Wright, A. E. *Angew. Chem., Int. Ed.* **2011**, *50*, 3219.
- (21) Zhang, Y.; Di, Y.-T.; Zhang, Q.; Mu, S.-Z.; Tan, C.-J.; Fang, X.; He, H.-P.; Li, S.-L.; Hao, X.-J. *Org. Lett.* **2009**, *11*, 5414.
- (22) Ding, L.; Maier, A.; Fiebig, H.-H.; Görls, H.; Lin, W.-H.; Peschel, G.; Hertweck, C. *Angew. Chem., Int. Ed.* **2011**, *50*, 1630.
- (23) Simunovic, V.; Müller, R. *ChemBioChem* **2007**, *8*, 1273.